Optics and Spectroscopy, 2024, Vol. 132, No. 9

18

Photoinduced change in diffusion coefficient as revealed by holographic relaxometry and laser scanning microscopy

© L.N. Borodina, V.N. Borisov, A.V. Veniaminov

International research and educational center for physics of nanostructures, ITMO University,
Saint-Petersburg, Russia

e-mail: lnborodina@itmo.ru

Received May 24, 2024
Revised September 25, 2024
Accepted September 25, 2024

We show that not only holographic relaxation, but also luminescence recovery studies of diffusion based on formation of photoinduced optical inhomogeneity and subsequent monitoring its relaxation reveal changes in the diffusion coefficients caused by exposure. This makes it possible to study photoinduced aggregation, destruction, and release of particles. Holographic relaxometry and modified fluorescence recovery after photobleaching techniques are outlined. Experimental examples of the luminescence recovery technique applied to colloid solutions of quantum dots are provided that cannot be described by simple Gaussian profile model. Possible variants of relaxation curves and spatial luminescence profiles reflecting photoinduced changes in diffusion mobility are simulated. Comparative study of diffusion in a model system using the two techniques is fulfilled.

Keywords: photoinduced grating relaxation, fluorescence recovery after photobleaching, photoinduced change in diffusion coefficient, confocal microscopy, supplementary gratings, camphoroquinone, quantum dots.

DOI: 10.61011/EOS.2024.09.60046.6730-24

Introduction

Nanoparticles and nanostructures are widely used in various applications of nanophotonics, optoelectronics, including lasers, photovoltaics, material engineering, sensor devices, catalysis and biomedicine [1–6]; they have crucial value in formation of holograms in both, modern photopolymers, and in silver-halide materials.‘ Along with the spectral properties of nanoparticles, information about their diffusion mobility is important, which, in particular, determines both the formation and destruction of holograms in polymer materials. [7]. The speed of particles motion is directly related to their size, and it can be used to evaluate their destruction, transformation, and aggregation. To determine the hydrodynamic sizes of particles by their mobility various optical and spectroscopic approaches are used based on statistics of scattered light fluctuations (dynamic light scattering, photon correlation spectroscopy [8]) or luminescence intensity (fluorescence correlation spectroscopy [9]), direct trajectory tracking, non-radiative energy transfer also assessed by spectra and intensity of luminescence. A separate group consists of methods where dynamics of the photoinduced spatial inhomogeneity is observed, e.g., fluorescence recovery after photobleaching and holographic relaxometry (holographic grating relaxation, forced Rayleigh scattering), which are very rarely applied to nanoparticles [10,11].

The study is aimed at comparing results on diffusion obtained by two methods using creation of optical inhomogeneity by means of light exposure and observation of subsequent changes by diffraction (holographic relaxation method) or luminescent (luminescence recovery method) response. A thorough knowledge of the microscopic mobility of molecules and nanoparticles obtained from formation and observation of concentration and related optical inhomogeneities, provides important information not only about the size of nanoparticles and the local viscosity of their environment, but also about the phototransformation of nanoparticles due to the changes in their diffusion and optical properties; as well as it also makes it possible to create efficient volumetric diffraction elements for augmented reality, distributed feedback lasers, holographic and luminescence sensors [5].

Materials and research methods

The following materials were used in the study: camphoroquinone (CQ, CAS 10373-78-1, Aldrich), 2-carboxyethyl acrylate (CAS 24615-84-7, Aldrich), phenolphthalein dimethyl ether (PDE, CAS 6315-80-6) synthesized in the Institute for Physical Chemistry (Johannes Gutenberg Universität Mainz, Germany). CQ solution in molten PDE 1 : 100 was placed between two cover slides 22×22 mm (Duran, Germany) and formed a transparent layer during cooling. CdSe/ZnS quantum dots with an average core diameter of 3.5 nm stabilized by trioctylphosphine oxide (TOPO) were synthesized by Dr. A. Dubavik in the International Scientific and Educational Center for Physics of Nanostructures of ITMO University according to the procedure described in [12,13].

To provide their colloidal stability in 2- carboxyethyl acrylate a method described in [14] was used.

To maintain the temperature of the samples, a temperature stabilizer Termodat 16 (Control Systems, Russia) and a thermally stabilized stage THMS600 (Linkam, Great Britain) were used.

The holographic relaxation experiment was performed using an optical system similar to that described in [15], equipped with a diode-pumped continuous-wave Nd:YAG laser with frequency doubling (532 nm); electromechanical shutters with a response time of at least 0.02 s and an avalanche photodiode photodetector SPCM-AQR (Perkin Elmer, Canada).

The modified method of fluorescence recovery after photobleaching sFRAP was implemented by using a laser scanning microscope LSM710 (Carl Zeiss Microimaging, Germany) with a 405 nm continuous-wave diode laser. The essence of the two optical methods of diffusion research is described below.

Method of holographic relaxometry

Method of holographic relaxometry [16–18], also known as holographic (grating) relaxation technique/spectroscopy [18–21], method of dynamic gratings [22] or transient gratings [23,24], forced Rayleigh scattering (FRS) [10,25], is based on the formation of periodic optical inhomogeneity (grating) in the studied material caused by exposure to an interference pattern (holographic recording) and monitoring the intensity of a probe light beam diffracted on such a structure. According to the change in this intensity after recording, it is possible to evaluate the processes that cause these changes, in particular, heat transfer, chemical processes, but above all diffusion.

When recording an interference pattern of two plane waves with a spatial intensity distribution in the studied material,

$$I(x,0)=\frac{I_m}{2}\left(1+\cos\left(\frac{2\pi x}{\Lambda}\right)\right) \qquad (1)$$

assuming the linearity of the recording, a one-dimensional harmonic spatial distribution is formed in it associated with the concentration of B product of photosensitive particles Aphoto-transformation;

$$C_B(x,0)=C_1\left(1+\cos\left(\frac{2\pi x}{\Lambda}\right)\right), \qquad (2)$$

this distribution repeats the light intensity spatial distribution in the interference pattern (1), and its anti-phase distribution of particles A that remains in the primary state

$$C_A(x,0)=C_0-C_1\left(1+\cos\left(\frac{2\pi x}{\Lambda}\right)\right), \qquad (3)$$

where C_0 stands for particles concentration before exposure, C_1 is amplitude of modulation of their concentration right after exposure to the interference field (recording of holographic grating), x — coordinate along the grating vector.

One-dimensional equation of diffusion with a constant coefficient

$$\frac{\partial C(x,t)}{\partial t}=D\,\frac{\partial^2 C(x,t)}{\partial x^2}, \qquad (4)$$

where D — diffusion coefficient, C — concentration, t — time, x — spatial coordinate at harmonic initial conditions (2), (3) indicates the cosine shape of distribution of components A and B:

$$C_A(x,0)=C_0-C_1\left(1+\cos\left(\frac{2\pi x}{\Lambda}\right)\exp\left(-\frac{4\pi^2 D_A t}{\Lambda^2}\right)\right),$$

$$C_B(x,0)=C_1\left(1+\cos\left(\frac{2\pi x}{\Lambda}\right)\exp\left(-\frac{4\pi^2 D_B t}{\Lambda^2}\right)\right).$$

Modulation amplitudes C_{1A} and C_{1B} of the obtained distributions decay exponentially with time because of the diffusion of particles A and B:

$$C_{1A,B}(t)=C_1\,\exp\left(-\frac{4\pi^2 D_{A,B} t}{\Lambda^2}\right)=C_1\exp(-t/\tau_{A,B}), \qquad (5)$$

where $D_{A,B}$ are diffusion coefficients of particles A and B, $\Lambda=\lambda/(2\sin\Theta)$ is spatial period defined by the convergence angle Θ of the interfering beams in the course of recording and their wavelength λ.

The characteristic relaxation times of these gratings $\tau_{A,B}=(\Lambda/2\pi)^2/D_{A,B}$ are inversely proportional to the diffusion coefficients of the particles in their initial and photo-transformed states and are generally different. Together with the optical parameters of the particles, they determine the observed evolution of the photoinduced grating. In the weak grating approximation, which is usually true for the holographic relaxometry, allowing to take into account neither the ratio of amplitude and phase contributions to the diffraction efficiency, nor the specific functions of the diffraction efficiency versus modulation [18], this evolution is delineated by the squared difference of two exponentials (5) [20]:

$$I(t)=I(0)[A\exp(-t/\tau_A)-B\exp(-t/\tau_B)]^2, \qquad (6)$$

where coefficients A and B describe contributions of the initial and photo-transformed particles, respectively, into the complex refractive index modulation of the medium. Depending on the ratio of characteristic time periods τ and coefficients A and B the relaxation curve (6) may be represented as one of three options(*1-3*) shown in Fig. 1. In cases *i* and *ii* the modulation of optical parameter associated with the light diffraction on the grating has a permanent sign, in *iii* this sign changes at some specific point moment of time, and the diffraction efficiency drops

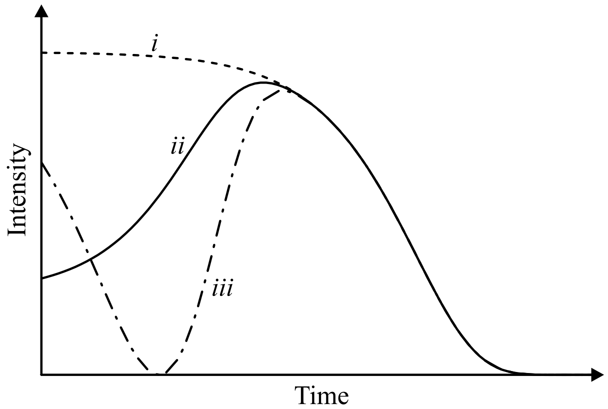

Figure 1. Three possible versions of the relaxation curves of the photoinduced gratings diffraction efficiency corresponding to the equation (6).

down to zero. If the photo-transformation changes the diffusion coefficient of the particle, then ii or iii cases apply.

Non-monotonic relaxation of the photo-induced grating caused by contributions of initial and transformed forms A and B, is known in the holographic relaxometry as a complementary grating effect [26].

In case of a nonlinear response of a material to light exposure caused by concentration saturation [15] or the combined action of a chemical reaction and multicomponent diffusion in photopolymerizable media with nanoparticles [27], a non-sinusoidal grating is formed, which is clearly visualized in a luminescent image when quantum dots (QD) are used as a neutral component [14,27]. When the grating thickness is sufficient to meet the conditions of Bragg diffraction, the relaxation of each spatial harmonic of such a grating can be recorded independently, taking into account the Bragg conditions for the corresponding harmonic component [15,28].

In some cases, for example, in spatially inhomogeneous media such as polymers near the glass transition temperature, the grating relaxation components deviate from pure exponential shape, but can be described by the stretched exponential (Kohlrausch function) [18]. Another manifestation of the spatial inhomogeneity of a medium may be nonlinear dependence of the grating relaxation rate on the squared spatial period; in this case, diffusion can be characterized by an apparent coefficient that depends on the spatial scale set by the grating period. Analysis of this dependence allows characterizing the medium inhomogeneity [29,30].

Luminescence technique for diffusion study

An optical approach to the study of diffusion, which is alternative to the holographic method and is also based on the analysis of changes in photoinduced inhomogeneity, is focused on the luminescent rather than diffraction signal.

The original version of fluorescence recovery after photobleaching (FRAP) technique consists in the local change of the photoluminescence (PL) efficiency (conventionally referred to as bleaching) in a microscopic region of the sample under exposure to intense light followed by further monitoring the intensity recovery in this region due to the spatial redistribution of particles with changed and initial PL efficiency [31,32].

The use of laser scanning microscopy allows for forming the optical inhomogeneities of almost arbitrary shape in the studied sample and analyzing not only the integral luminescence intensity, but also the redistribution of luminescence intensity in space over time [33–36]. This makes it possible to determine not only the diffusion coefficient but even, for example, the apparent diffusion dimension [33], as well as take into account any possible gradual discoloration of the sample caused by luminescence-exciting radiation and visualize the spatially inhomogeneous pattern.

Reduction to one-dimensional diffusion is convenient for measuring and analyzing the results. To neglect the effect of diffusion in axial direction, the sample thickness shall not be large compared to the depth of field of the optical system, and the formation of a stripe-shaped inhomogeneity also excludes diffusion along it, leaving only lateral diffusion in the transverse direction. Such version of FRAP method may be named *Stripe*-FRAP (sFRAP).

The solution of the one-dimensional equation (3) with an initial condition corresponding to a x_c symmetrical stripe with a width of $2h$, represents itself a sum of two error functions:

$$C(x,t)=\frac{C_0}{2}\left(\operatorname{erf}\left(\frac{h+x-x_c}{2\sqrt{Dt}}\right)+\operatorname{erf}\left(\frac{h-x+x_c}{2\sqrt{Dt}}\right)\right), \tag{7}$$

approaching the Gaussian function, the fundamental solution of the diffusion equation describing diffusion from a point source,

$$C(x,t)=C_0\frac{\exp\left(-\frac{(x-x_c)^2}{4Dt}\right)}{2\sqrt{\pi Dt}}=C_0\frac{\exp\left(-\frac{(x-x_c)^2}{2\langle\Delta x^2\rangle}\right)}{2\pi\langle\Delta x^2\rangle}, \tag{8}$$

the faster, the narrower is the original stripe relative to a root-mean-square displacement of the diffusing particles $\sqrt{\langle\Delta x^2\rangle}=\sqrt{2Dt}$.

Then, assuming the linearity of the luminescent response, which implies low absorption and independence of the luminescence quantum yield from concentration, the luminescence intensity distribution in the direction perpendicular to a fairly narrow exposed stripe is described by

$$I(x,t)=I_0+A\,\frac{\exp\left(-\frac{2(x-x_c)^2}{w^2}\right)}{w\sqrt{\pi/2}}, \tag{9}$$

where $\omega=2\sqrt{2Dt}=2\sqrt{\langle x^2\rangle}$ is the parameter of the Gaussian profile width. Its square physically means a fourfold mean square of the particles diffusive displacement during t

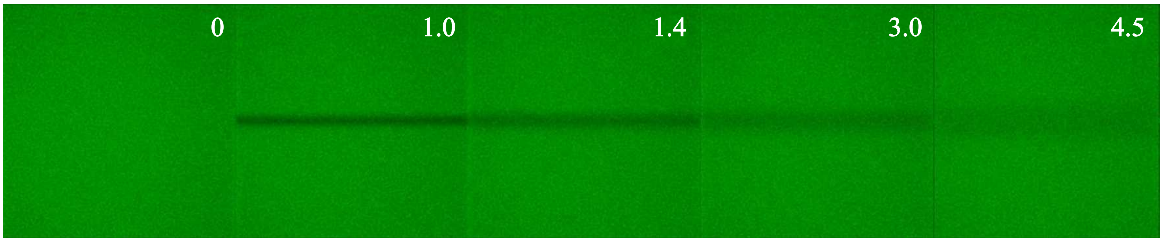

Figure 2. Luminescent images of $850 \times 850\,\mu$m region of quantum dots colloidal solution in hexane (0, leftmost image) and in 1−4.5 s after the stripe-shaped exposure. Gradual expansion and disappearance of the stripe are noticeable caused by the diffusion mixing of the QD solution.

under one-dimensional diffusion and is proportionate to the diffusion coefficient D:

$$w^2 = 8Dt = 4\langle x^2\rangle. \tag{10}$$

From Stokes−Einstein formula [37]

$$D = \frac{k_B T}{6\pi\eta r}, \tag{11}$$

where k_B is Boltzmann constant, T is absolute temperature, it is possible to define the size of the particles, if we know viscosity of the solvent η or visa versa, find the apparent viscosity of the environment knowing the size of the diffusing particles. This allows us to evaluate the transformations, aggregation, release, destruction of particles, micro-viscosity and the degree of uniformity of their environment, and tracking the displacement of the coordinate of the center of the Gaussian contour x_c provides with information about particle drift, for example, in a magnetic [38,39] or electric field.

However, until recently, the possibility of simultaneous, in a single experiment, investigation by the luminescent method of diffusion of the original and photo-transformed forms of particles, similar to a possibility provided by the effect of complementary gratings in holographic relaxometry, was neither mentioned nor used. The next section presents the results of experiments with colloidal quantum dots, indicating this possibility.

Example of luminescence recovery for quantum dots in colloid solution

To study the nanoparticles diffusion by sFRAP method using a scanning laser beam of the confocal laser scanning microscope LSM710 (Carl Zeiss Microimaging, Germany) a narrow $20\,\mu$m stripe (oriented along the lines) of CdSe/ZnS QDs colloidal solution in hexane was exposed; for this purpose the solution was placed into a 1 mm quartz cell in such a way that the intensity of luminescence in it is decreased by 10−20 % from the initial value. Exposure was carried out through the lens 10x/0.2 by emitting the 405 nm diode laser with a power of 1 mW.

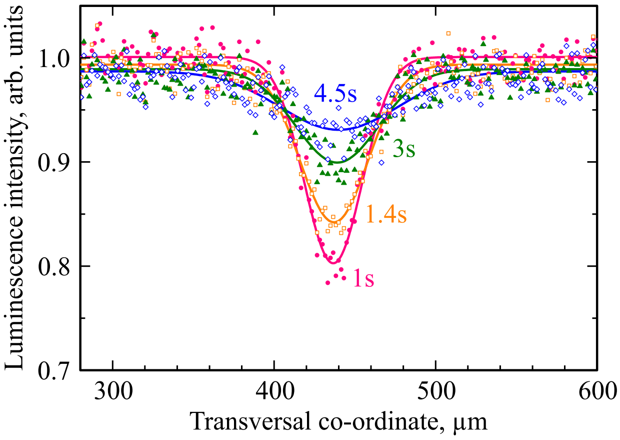

Figure 3. Transverse luminescent patterns of QD solution in 1−4.5 s after exposure, normalized to the original profile (dot) (before exposure), and the results of their Gaussian approximation (curves).

A higher change in the luminescence intensity would probably increase the image contrast and signal-to-noise ratio, but it would require a long exposure, and as a result, information about the initial relaxation phase would be lost.

Both, before and after exposure, with a frequency depending on the rate of change in the intensity distribution, luminescent images of a solution area with a stripe were captured when scanning with attenuated ($30\,\mu$W) laser radiation to minimize any additional bleaching. Some of such images obtained after various periods of time after exposure are shown in Fig. 2.

To increase the signal-to-noise ratio, the luminescence intensity was averaged over several hundred columns along the exposed stripe. As a result, for each frame, a one-dimensional intensity distribution was obtained along the coordinate perpendicular to the stripe (Fig. 3), which is then normalized to the original distribution and approximated by the Gaussian function (9) to compensate for possible intensity inhomogeneity.

Calculated from the slope of a linear dependence of w^2 on time, the diffusion coefficient $350 \pm 30\,\mu\text{m}^2$/s

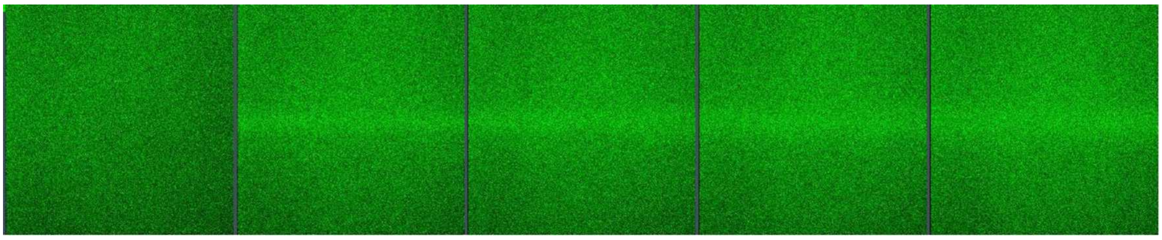

Figure 4. Sequential luminescent images of QD colloidal solution in hexane, demonstrating the expansion of a bright PL stripe formed in the exposed area.

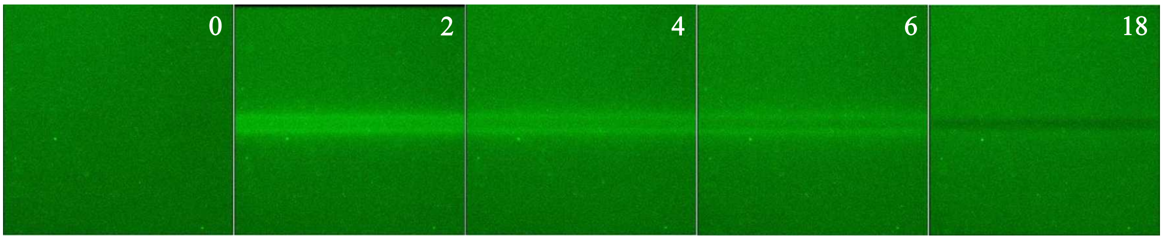

Figure 5. Luminescent images of 425 × 425 μm region of colloidal solution of QD in 2-carboxyethyl acrylate before exposure (0) and in 2, 4, 6, 18 s after exposure, demonstrating separation of the exposed stripe in two stripes with a black stripe between them that obviously cannot be described by a single Gaussian function.

corresponds to the diffusion of spherical particles with a hydrodynamic radius of 2.0 ± 0.2 nm.

Conventional name of FRAP method implies a decrease in luminescence intensity as a result of a decrease in the quantum yield or the number of luminescent centers under high-intensity exposure to laser radiation, referred to as photobleaching. For the luminescent semiconductor nanocrystals, such as QDs, both are typical: the decrease in photo-luminescence quantum yield (Fig. 2) and its increase (photo-activation observed at relatively small exposures as shown in Fig 4)[40]. Surely, this doesn't hinder the diffusion coefficient to be determined from expanding Gaussian luminescence intensity profiles.

However, the shape of the PL profile observed in a number of experiments is clearly not described by the simple representation (9), (10) of the diffusion of particles differing only in the quantum yield of PL. The representative example of the sequentially observed PL QDs patterns in 2-carboxyethyl acrylate is shown in Fig. 5.

It is possible that the change in the quantum yield of luminescence as a result of exposure does not exhaust the factors determining the shape and width of the spatial profile of its intensity.

It is known that photochemical transformations of molecular probes lead to significant changes in their mobility. For example, according to holographic relaxation measurements, the diffusion coefficient of camphoroquinone molecules in polycarbonate at temperatures near the glass transition temperature decreases more than tenfold upon addition of a hydrogen atom in a photochemical reaction which, apparently, could not lead to a significant increase in molecular volume [41]. The diffusion coefficient changes even more drastically — by orders of magnitude — when phenanthrenequinone is photoattached to the macromolecules of polymethyl methacrylate, which can be used to create self-manifesting highly selective holographic elements [42]. The possibility of changing the diffusion properties should now be taken into account, along with changes in the quantum yield of PL, when considering the results of luminescent measurements.

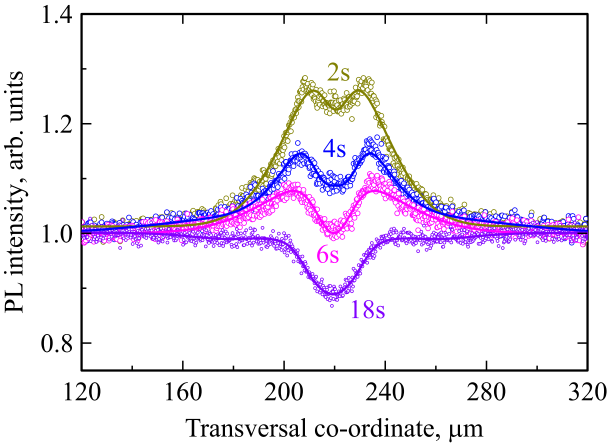

Figure 6. Transverse profiles of PL images intensity as shown in Fig. 5, normalized at initial profile (dot), and results of their approximation (lines) by the function (12).

Then, the spatial profile of the luminescence intensity will be defined not by the Gaussian function, but by the difference of such functions (with a common center) one of which is responsible for distribution of luminescent centers

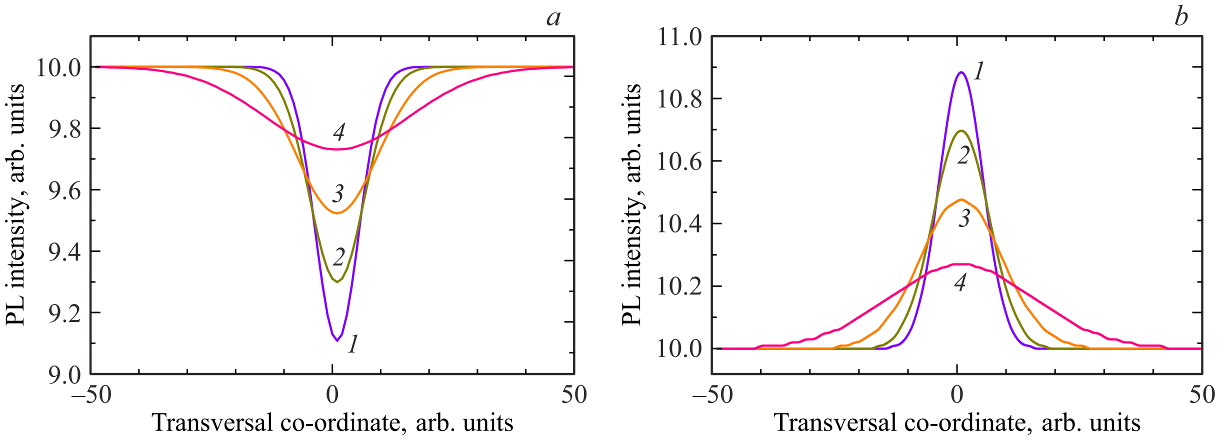

Figure 7. Sequences of luminescent profiles in the direction perpendicular to the exposed stripe, calculated using formula (12) for cases of a decrease (*a*) and an increase (*b*) in the luminescence quantum yield by 10% as a result of exposure. The numbering of the curves corresponds to the sequence of the profiles over time.

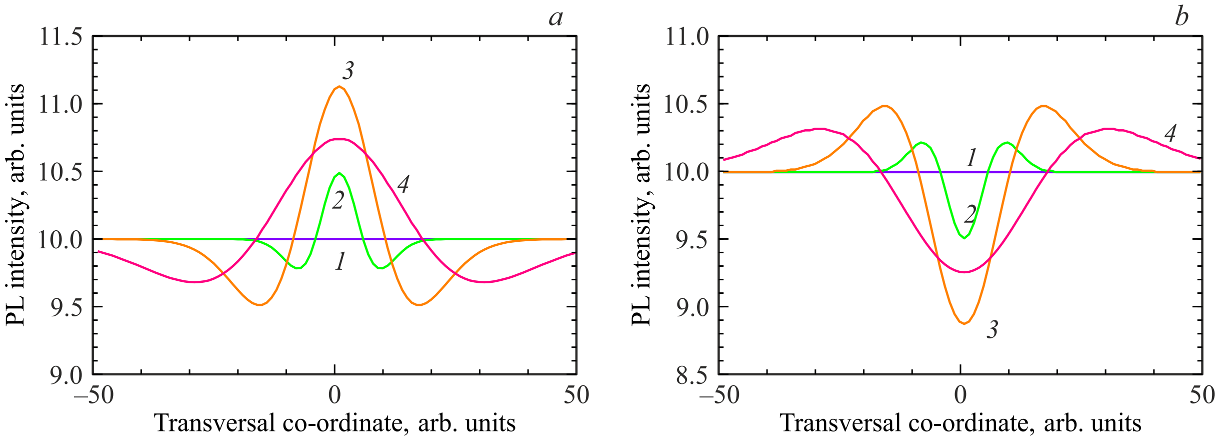

Figure 8. Examples of luminescence profiles for cases of double deceleration (*a*) and acceleration(*b*) of diffusion during exposure without changing the luminescence quantum yield. The numbering of the curves corresponds to the sequence of the profiles over time.

in their initial state *A*, and the other one — in the photo-transformed state *B*; their constants are defined by the quantum yield of PL, absorbance of excitation light and degree of transformation of *A* in *B*. The width of each of these Gaussian functions will change with a rate defined by the diffusion coefficient $D_{A,B}$ of particles *A* and *B*, similar to (9).

$$I(x,t) = I_0 + B\,\frac{\exp\left(-\frac{(x-x_c)^2}{4D_B t}\right)}{2\sqrt{\pi D_B t}} - A\,\frac{\exp\left(-\frac{(x-x_c)^2}{4D_A t}\right)}{2\sqrt{\pi D_A t}}. \qquad (12)$$

Indeed, expression (12) accurately describes the profiles of the PL intensity distributions shown in Fig.5 (Fig. 6).

In contrast to the mixtures of particles of various sizes considered in the paper [43], the mixture of original and photo-transformed particles formed during exposure in sFRAP experiments in this study generates the opposite concentration profiles and shall be considered separately.

Modeling of changes in the spatial profile of luminescence

In order to illustrate what possible combinations of changes in the quantum yield of luminescence and particles diffusion coefficient can manifest themselves in the experiments, the development of the luminescence intensity spatial distribution as a result of one-dimensional diffusion was simulated using the Mathcad software. Fig. 7 illustrates the results of intensity profiles calculation by formula (12) for the case of photo-induced decrease (bleaching) (*a*) and increase (photo-activation) (*b*) of the luminescence quantum yield without changing the diffusion coefficient.

Fig. 8 depicts the photo-induced decrease (*a*) and increase (*b*) in the diffusion coefficient without changing the PL quantum yield are considered. In this situation, there is no inhomogeneity of PL intensity immediately after exposure (line *1* in Fig. 8), it appears over time as a bright

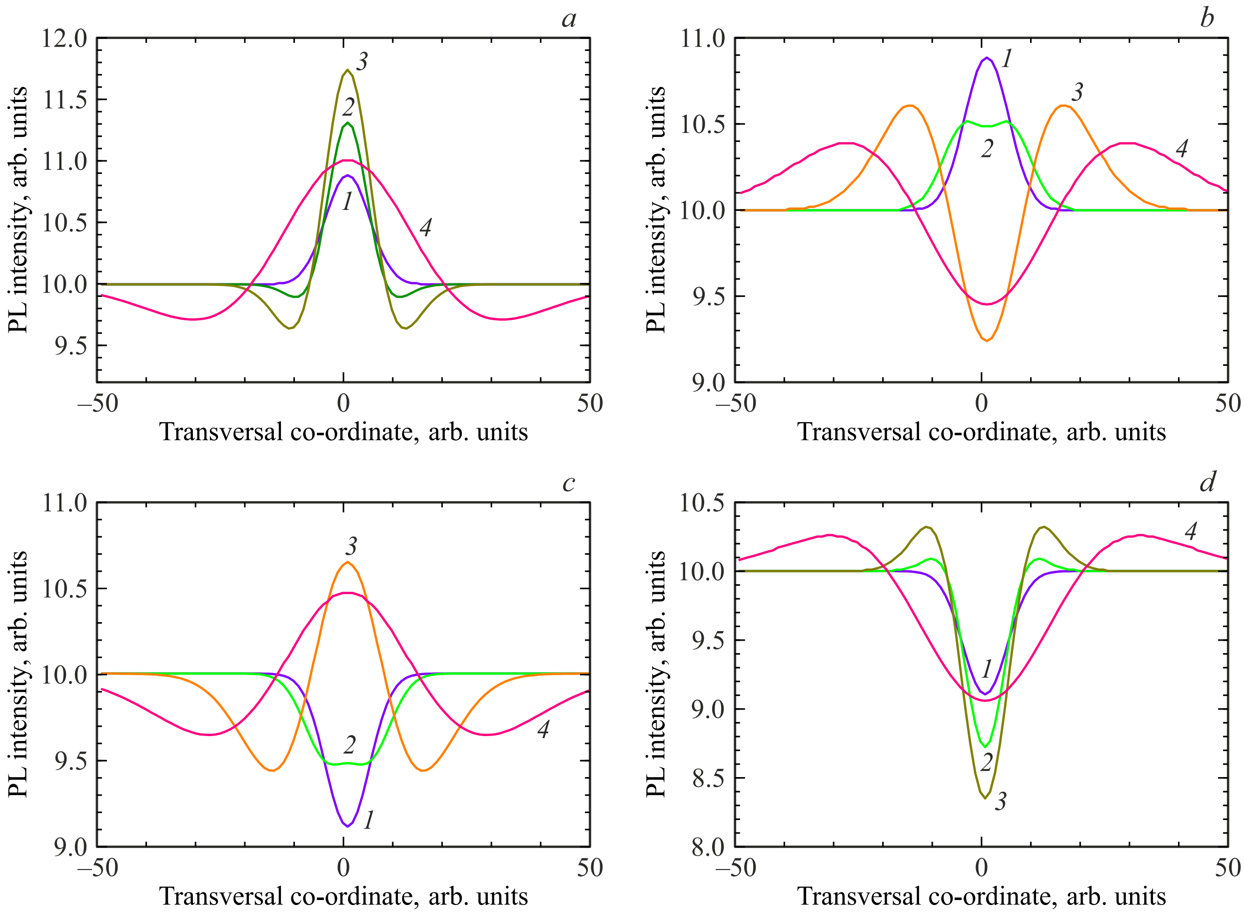

Figure 9. Examples of luminescence profiles for increase (a, b) and decrease (c, d) of its quantum yield at deceleration (a, c) and acceleration (b, d) of diffusion, calculated by formula (12). The numbering of the curves corresponds to the sequence of the profiles over time.

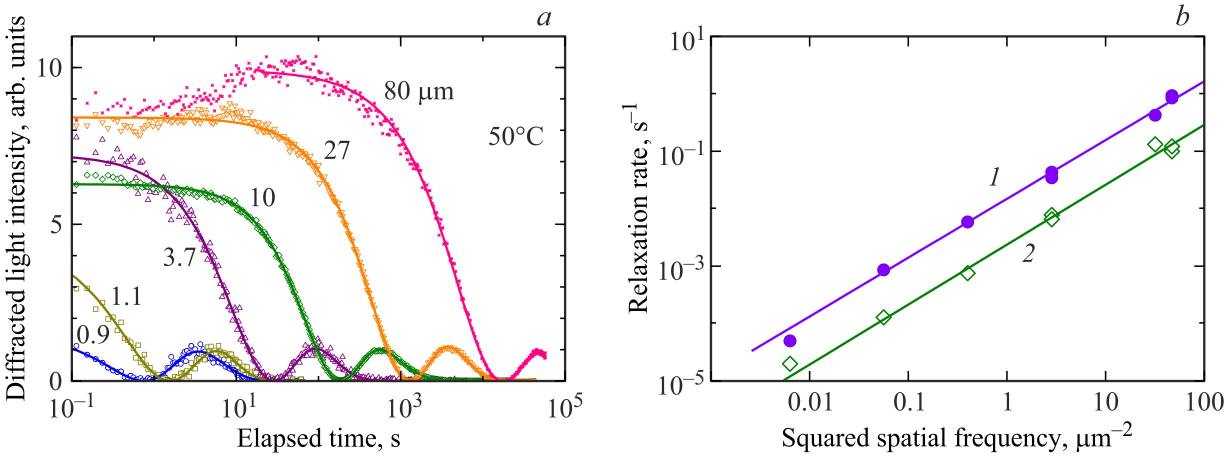

Figure 10. Relaxation curves of photoinduced gratings with spatial periods 0.9−80 μm recorded in CQ-PDE compositions at 50 °C (a) and the dependences of the speed constants of their fast (1) and slow (2) relaxation components on the squared spatial frequency (b).

band between two dark ones (Fig. 8, a) or dark between two bright ones (Fig. 8, b), with the difference between the intensity of the PL the stripes and background change non-monotonously.

Thus, the implementation of the diffusion mobility research method, which was originally based on photobleaching and has this word in its name (Fluorescence Recovery After Photobleaching), is possible without the

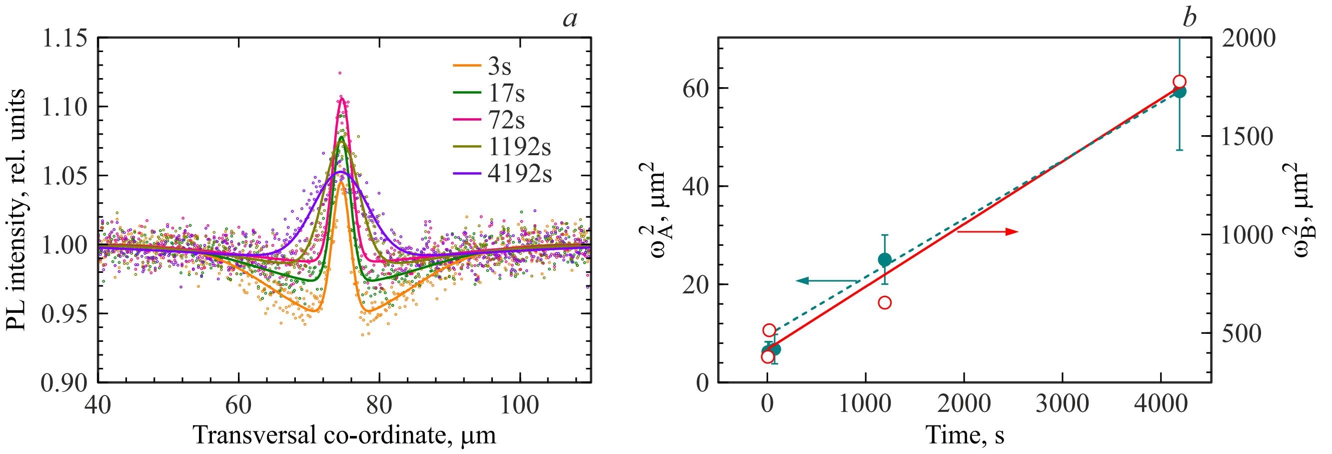

Figure 11. Sequences of CQ luminescence intensity profiles in PDE (in the direction perpendicular to the exposed stripe) obtained in different periods of time after being exposed at the wavelength of 405 nm at 50°C with the use of a laser scanning microscope, lines — results of their approximation by a difference of two Gaussian functions with a common center (12) (*a*); squared width of the Gaussian functions versus time (*b*).

bleaching itself, i.e. without changing the quantum yield of luminescence.

More general cases of simultaneous changes in the quantum yield of PL and the diffusion coefficient are shown in Fig. 9. The family of curves standing for simultaneous growth (*b*) and decrease (*c*) of the luminescence quantum yield and diffusion coefficient, are qualitatively symmetrical relative to each other, similar to the profiles family observed during PL growth with diffusion deceleration (*a*) and during decrease of PL with diffusion acceleration (*d*). However, change of diffusion properties is noticed in the luminescence profiles, only if both forms of the substance *A* and *B* are luminescent, otherwise the profile and its variation are defined only by the luminescent form *A* or *B*.

Thus, all possible situations of changes in the diffusion coefficient and quantum yield of PL, which can be obtained in sFRAP experiments, were modeled. The situation observed in series of sFRAP experiments with colloidal QDs in a monomeric medium (Fig. 6) qualitatively corresponds to the modeled situation describing simultaneous increase in both the quantum yield of PL and the diffusion coefficient of nanocrystals (Fig. 9, *b*).

Experimental check of the diffusion coefficient variation

To verify the idea of the photoinduced change in diffusion mobility, comparative experimental studies of camphoroquinone (CQ) diffusion in phenolphthalein dimethyl ether (PDE) using holographic relaxometry and sFRAP luminescence recovery were conducted. Measurements were carried out at 50–70°C in PDE melt, the glass transition temperature of which is 21°C. The relaxation properties of PDE are given in details in article [44].

The results of previous holographic relaxation studies indicated the change in the diffusion mobility of camphoroquinone during its photoreduction in polymer systems [28], while PDE was earlier used as a matrix for the photosensitive systems subjected to holographic relaxation studies [45], and the photoreduction of phenanthrenequinone in it was successful [15]. The methyl groups of PDE act as a source of protons and participate in photo-reduction of CQ.

The holographic relaxation experiment was performed using an optical system similar to that described in [15], equipped with a diode-pumped continuous-wave Nd:YAG laser with frequency doubling, electromechanical shutters with a response time of at least 0.1 s and an avalanche photodiode photodetector SPCM-AQR (Perkin Elmer, Canada). In the samples placed between the cover slides, an interference pattern of two beams with a diameter of about 1 mm was recorded, forming a transmission grating with a spatial period of 0.9–80 μm, depending on the angle between the recording beams.

Fig. 10, *a* shows the light intensity versus time dependences measured at 50°C for the light diffracting on the photo-induced gratings (in terms of shape they obviously relate to case *iii* Fig. 1), and in Fig. 10, *b* depicts the relaxation rates as a function of the squared spatial frequency obtained from the analysis of these curves.

For clarity, the dependencies are shown in Fig.10, *b* on a logarithmic scale, although the slope of the dependence on a linear scale is used to determine the diffusion coefficient. From this data we have found the diffusion coefficients 0.015 ± 0.004 and $0.0024 \pm 0.0006\,\mu\text{m}^2/\text{s}$, where the largest coefficient stands for CQ, and the lowest coefficient stands for the photo-reduction product based on the assumption, that the latter has larger amount of atoms and, therefore, may have larger volume.

In the course of sFRAP luminescence experiments conducted in the temperature range of 50–70°C, sequences of

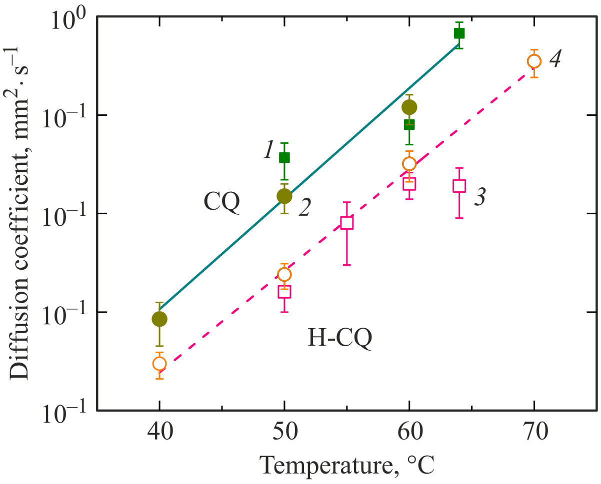

Figure 12. Diffusion coefficients of CQ (dark symbols *1, 2*) and its photo-transformation product H-CQ (light symbols *3, 4*) in PDE at various temperatures measured by holographic (squares *1, 3*) and luminescent (circles *2, 4*) methods; results of linear approximation of data for CQ (solid line) and H-CQ (dashed line) are given for better perception.

luminescent profiles were obtained, an example of which related to the temperature 50°C is shown in Fig. 11, *a*. In contrast to the results of holographic relaxometry, from the luminescent profiles we may clearly see that the diffusion coefficient of the photo-product, the concentration of which is is increased in the illuminated stripe, is lower than that of the original form of CQ. This confirms the assumption made during the discussion related to Fig. 10. The quantum yield of the photoproduct luminescence is higher than that of CQ itself. The profiles are qualitatively consistent with the situation shown in Fig. 9, *a*.

Dependencies of the squared Gaussian width of the complex profile components (obtained through approximation of data in Fig. 11, *a* by formula (12)), on time are given in Fig. 11, *b*. Based on the slope of these dependencies the diffusion coefficients 0.037 ± 0.015 and $0.0016 \pm 0.0008\,\mu m^2/s$, were found relatively close to the values obtained by holographic technique.

The results of measuring the diffusion coefficient of CQ and its photo-transformation product H-CQ at various temperatures are shown in Fig.12.

By comparing the temperature dependences of the diffusion coefficients shown in Fig. 12, it can be stated with confidence that the results obtained by these two optical methods have good mutual correlation.

Conclusion

Similar to complementary gratings in holographic relaxometry, the evolution of the spatial profile of luminescence intensity used to study diffusion by means of luminescence recovery after photobleaching is influenced by changes in the diffusion coefficient of particles caused by exposure. Information about diffusion coefficients of both the original and photo-transformed forms is contained also in the relaxation curves of the diffraction efficiency and, as newly noticed, in the luminescence intensity profiles. At the same time, the actual bleaching (change in the quantum yield of luminescence), on which the basic method of luminescence recovery and its very name are based, is no longer necessary for the implementation of the method. The two optical methods mutually confirm the adequacy of the results obtained with their help and the reality of the change in diffusion coefficients under light exposure.

Acknowledgments

The authors express their gratitude to the shared resources center „Nanotechnologies“ of ITMO University and the scientific and educational Center of Photonics and Optical Informatics of ITMO University for the opportunity to use their experimental equipment.

Funding

This study by L.B. was supported financially by the grant of NIRMA PT MF ITMO University.

Conflict of interest

The authors declare that they have no conflict of interest.

References

[1] I.V. Martynenko, A.P. Litvin, F. Purcell-Milton, A.V. Baranov, A.V. Fedorov, Y.K. Gun'ko. J. Mater. Chem. B, **5**, 6701–6727 (2017). DOI: 10.1039/C7TB01425B

[2] A.L. Efros, L.E. Brus. ACS Nano, **15**, 6192–6210 (2021). DOI: 10.1021/acsnano.1c01399

[3] *Nanocrystal quantum dots*, ed. by V.I. Klimov (CRC Press, 2017). DOI: 10.1201/9781420079272

[4] T.O. Oskolkova, A.A. Matiushkina, L.N. Borodina, E.S. Smirnova, A.I. Dadadzhanova, F.A. Sewid, A.V. Veniaminov, E.O. Moiseeva, A.O. Orlova. ChemNanoMat, **10**, e202300469 (2024). DOI: 10.1002/CNMA.202300469

[5] A.K. Yetisen, I. Naydenova, F. Da Cruz Vasconcellos, J. Blyth, C.R. Lowe. Chem. Rev., **114**, 10654–10696 (2014). DOI: 10.1021/cr500116a

[6] K.A. Altammar. Front. Microbiol., **14**, 1155622 (2023). DOI: 10.3389/fmicb.2023.1155622

[7] J.T. Sheridan, R.K. Kostuk, A.F. Gil, Y. Wang, W. Lu, H. Zhong, Y. Tomita, C. Neipp, J. Francés, S. Gallego, I. Pascual, V. Marinova, S.H. Lin, K.Y. Hsu, F. Bruder, S. Hansen, C. Manecke, R. Meisenheimer, C. Rewitz, T. Rölle, S. Odinokov, O. Matoba, M. Kumar, X. Quan, Y. Awatsuji, P.W. Wachulak, A.V. Gorelaya, A.A. Sevryugin, E.V. Shalymov, V.Yu. Venediktov, R. Chmelik, M.A. Ferrara, G. Coppola, A. Márquez, A. Beléndez, W. Yang, R. Yuste, A. Bianco, A. Zanutta, C. Falldorf, J.J. Healy, X. Fan, B.M. Hennelly, I. Zhurminsky, M. Schnieper, R. Ferrini, S. Fricke, G. Situ, H. Wang, A.S. Abdurashitov, V.V. Tuchin,

N.V. Petrov, T. Nomura, D.R. Morim, K. Saravanamuttu. J. Optics, **22**, 123002 (2020). DOI: 10.1088/2040-8986/abb3a4

[8] *Dynamic Light Scattering. Applications of Photon Correlation Spectroscopy*, ed. by R. Pecora (Plenum Press, New York and London, 1985).

[9] E. Haustein, P. Schwille. In: *Soft Matter Characterization*, ed. by R. Pecora (Springer, 2008), p. 637–675. DOI: 10.1007/978-1-4020-4465-6_11

[10] W. Schärtl. In: *Soft Matter Characterization*, ed. by R. Pecora (Springer, 2008), p. 678–701. DOI: 10.1007/978-1-4020-4465-6_12

[11] A.A. Moud. ACS Biomater. Sci. Eng., **8**, 1028–1048 (2022). DOI: 10.1021/acsbiomaterials.1c01422 12.

[12] D.V. Talapin, A.L. Rogach, A. Kornowski, M. Haase, H. Weller. Nano Lett., **1**, 207–211 (2001). DOI: 10.1021/nl0155126

[13] B.O. Dabbousi, J. Rodriguez-Viejo, F.V. Mikulec, J.R. Heine, H. Mattoussi, R. Ober, K.F. Jensen, M.G. Bawendi. J. Phys. Chem. B, **101**, 9463–9475 (1997). DOI: 10.1021/jp971091y

[14] L. Borodina, V. Borisov, K. Annas, A. Dubavik, A. Veniaminov, A. Orlova. Materials, **15**, 8195 (2022). DOI: 10.3390/MA15228195

[15] A.V. Veniaminov, H. Sillescu. Chem. Phys. Lett., **303**, 499–504 (1999). DOI: 10.1016/S0009-2614(99)00257-2

[16] E.I. Shtyrkov. *In book.: Problemy golographii* (M., 1973) (in Russian), v. 2, p. 258–262.

[17] A.V. Veniaminov, G.I. Lashkov, O.B. Ratner, N.S. Shelekhov, O.V. Bandyuk. Opt. Spectrosc., **60**, 87–91 (1986).

[18] A.V. Veniaminov, E. Bartsch, Opt. Spectrosc, **101** (2) 290–298 (2006). DOI: 10.1134/S0030400X06080182.

[19] X.R. Zhu, D.J. McGraw, J.M. Harris. Anal. Chem., **64**, (1992). DOI: 10.1021/ac00038a716

[20] C.S. Johnson. J. Chem. Phys., **81**, 5384–5388 (1984). DOI: 10.1063/1.447682

[21] J. Zhang, C.H. Wang. J. Phys. Chem., **90**, 2296–2297 (1986). DOI: 10.1021/j100402a006

[22] A.L. Tolstik, E.V. Ivakin, I.G. Dadenkov. Nonlinear Phenomena in Complex Systems, **26** (3), 73–283 (2023). DOI: 10.5281/zenodo.10034399

[23] J.T. Fourkas, M.D. Fayer. Acc. Chem. Res., **25**, 227–233 (1992). DOI: 10.1021/AR00017A004

[24] P. Bartolini, A. Taschin, R. Eramo, R. Torre. In: *Time-Resolved Spectroscopy in Complex Liquids* (Springer, 2007), p. 129–184. DOI: 10.1007/978-0-387-25558-3_3

[25] H.J. Eichler. In: *Festkörperprobleme*, ed. by J. Treusch (Springer, Berlin, Heidelberg, 1978), v. 18, p. 241–263. DOI: 10.1007/BFb0107784

[26] S. Park, J. Sung, H. Kim, T. Chang. J. Phys. Chem., **95**, 7121–7124 (1991). DOI: 10.1021/j100172a004

[27] Y. Tomita, E. Hata, K. Momose, S. Takayama, X. Liu, K. Chikama, J. Klepp, C. Pruner, M. Fally. J. Mod. Opt., **63**, S1–S31 (2016). DOI: 10.1080/09500340.2016.1143534

[28] T.K. Gaylord, R. Magnusson. JOSA, **67**, 1165–1170 (1977). DOI: 10.1364/JOSA.67.001165

[29] E. Bartsch, T. Jahr, A. Veniaminov, H. Sillescu. J. Phys. France IV, **10**, Pr7-289-Pr7-293 (2000). DOI: 10.1051/jp4:2000758

[30] A. Veniaminov, T. Jahr, H. Sillescu, E. Bartsch. Macromolecules, **35**, 808–819 (2002). DOI: 10.1021/ma010531n

[31] M. Carnell, A. Macmillan, R. Whan. Methods Mol. Biol., **1232**, 255–271 (2015). DOI: 10.1007/978-1-4939-1752-5_18

[32] N. Lorén, J. Hagman, J.K. Jonasson, H. Deschout, D. Bernin, F. Cella-Zanacchi, A. Diaspro, J.G. McNally, M. Ameloot, N. Smisdom, M. Nydén, A.M. Hermansson, M. Rudemo, K. Braeckmans. Quart. Rev. Biophys., **48**, 323–387 (2015). DOI: 10.1017/S0033583515000013

[33] S. Seiffert, W. Oppermann. J. Microscopy, **220**, 20–30 (2005). DOI: 10.1111/j.1365-2818.2005.01512.x

[34] Y. Cheng, R.K. Prud'homme, J.L. Thomas. Macromolecules, **35**, 8111–8121 (2002). DOI: 10.1021/ma0107758

[35] U. Kubitscheck, P. Wedekind, R. Peters. Biophys. J., **67**, 948–956 (1994). DOI: 10.1016/S0006-3495(94)80596-X

[36] K. Hashlamoun, Z. Abusara, A. Ramírez-Torres, A. Grillo, W. Herzog, S. Federico. Biomech. Model. Mechanobiol., **19**, 2397–2412 (2020). DOI: 10.1007/s10237-020-01346-z

[37] A. Einstein, M. Smolukhovsky. *Braunovskoye dvizhenie* (ONTI, 1934).

[38] L.N. Borodina. In book.: *Bulletin of abstracts of SRS of the University's graduates* (ITMO University, SPb., 2022), v. 1, p. 358–363.

[39] L. Borodina, A. Matyushkina, I. Vovk, A. Dubavik, A. Veniaminov, A. Orlova. In: *International Symposium Fundamentals of Laser Assisted Micro- & Nanotechnologies (FLAMN-22)* (ITMO, SPb, 2022), p. 16.

[40] O.V. Chashchikhin, M.F. Budyka. J. Photochem. Photobiol. A Chem., **343**, 72–76 (2017). DOI: 10.1016/j.jphotochem.2017.04.028

[41] C.H. Wang, J.L. Xia. Macromolecules, **21**, 3519–3523 (1988). DOI: 10.1021/ma00190a031

[42] A.V. Veniaminov, U.V. Mahilny. Opt. Spectrosc., **115** (6), 906–930 (2013). DOI: 10.1134/S0030400X13120199.

[43] G.I. Hauser, S. Seiffert, W. Oppermann. J. Microsc., **230**, 353–362 (2008). DOI: 10.1111/j.1365-2818.2008.01993.x

[44] F. Stickel, E.W. Fischer, R. Richert. J. Chem. Phys., **104**, 2043–2055 (1996). DOI: 10.1063/1.470961

[45] G. Heuberger, H. Sillescu. J. Phys. Chem., **100**, 15255–15260 (1996). DOI: 10.1021/jp960968a

Translated by T.Zorina